TISSUE ENGINEERING: Part A
Volume 00, Number 00, 2018

DOI: 10.1089/ten.tea.2018.0052

termis
Tissue Engineering
& Regenerative Medicine
International Society

Preclinical Optimization of a Shelf-Ready, Injectable, Human-Derived, Decellularized Allograft Adipose Matrix

Giorgio Giatsidis, MD, PhD,[1] Julien Succar, MD,[1] Anthony Haddad, MD,[1] Gianluigi Lago, MD,[1] Clara Schaffer, MD,[1] Xingang Wang, MD,[1,2] Benjamin Schilling, MS,[3] Evangelia Chnari, PhD,[4] Hajime Matsumine, MD, PhD,[1] and Dennis Paul Orgill, MD, PhD[1]

Autologous adipose tissue grafting is a popular strategy for soft tissue reconstruction; yet its clinical outcomes are often suboptimal. Lack of metabolic and architectural support at recipient sites affects the capacity of cellularized autologous grafts to survive after transplantation. Allograft adipose matrices (AAMs) are composed of extracellular matrices of adipose tissue. They can provide critical biophysical cues and create a supportive microenvironment for autologous graft survival. Using murine models, we have optimized the *in vivo* use of an injectable AAM obtained from human cadaveric tissue and processed to remove lipid and cellular components. We hypothesized that the AAM could assist recipient site preparation before autologous adipose tissue grafting and—alone or combined with other treatments—improve surgical outcomes. The AAM scaffolds retained volume (measured as cross-sectional area at histology) over time and showed a higher local angiogenesis. Preconditioning of AAM recipient sites using intermittent external volume expansion further increased their vascularity and promoted adipogenesis. Low-density AAM combined with autologous adipose tissue grafts best assisted angiogenesis and tissue survival. These studies demonstrate that the AAM contributes to recipient site preparation before or in combination with autologous adipose tissue grafting by increasing vascularity and by creating an adipogenic microenvironment. This patient-ready scaffold could help improve outcomes in soft tissue reconstructive surgery.

Keywords: adipose tissue engineering, decellularized matrix, angiogenesis, adipogenesis, allograft, soft tissue reconstruction and regeneration

Impact Statement

Trauma, disease, surgery, or congentital defects can cause soft tissue losses in patients, leading to disfigurement, functional impairment, and a low quality of life. In the lack of available effective methods to reconstruct these defects, acellular adipose matrices could provide a novel therapeutic solution to such challenge.

Introduction

AUTOLOGOUS, cellularized adipose tissue grafting has become a popular technique for soft tissue reconstruction due to its ability to provide a natural outcome through a minimally invasive procedure.[1–3] The technique has proven to be very effective in restoring small- and medium-volume defects, but it has shown limited outcomes in the reconstruction of large-volume defects.[4–6]

The lack of an adequate metabolic (vascular) and architectural (extracellular matrix or ECM) support for cellularized grafts at the recipient sites has been identified as the two leading

[1]Tissue Engineering and Wound Healing Laboratory, Division of Plastic Surgery, Department of Surgery, Brigham and Women's Hospital, Harvard Medical School, Boston, Massachusetts.
[2]Department of Burns and Wound Care Center, Second Affiliated Hospital of College of Medicine, Zhejiang University, Hangzhou, China.
[3]Department of Bioengineering, School of Bioengineering, University of Pittsburgh, Pittsburgh, Pennsylvania.
[4]Musculoskeletal Transplant Foundation, Edison, New Jersey.

causes of this phenomenon.[4,6–8] Optimization of the recipient site or ''niche'' of the autologous graft is a pivotal strategy to assist tissue engraftment and long-term survival.[9–19]

Allograft and xenograft ECM-biomimetic scaffolds have proven to be an effective tool for promoting tissue repair and regeneration (such as skin) in numerous preclinical and clinical studies.[20–24] Several studies have previously shown that biomimetic scaffolds (that induce adipogenesis and adipose tissue regeneration) can be obtained through decellularization of adipose tissue.[13,15,16,19,25–29] Numerous studies have investigated the biological properties of decellularized adipose tissue obtained from nonhuman sources: although these studies can provide important experimental insights, direct application to patients is unfeasible within a short-term period due to limited availability (rodents and smaller animals) or the possible presence of immunological mismatch that could cause rejection (swine). Yet, several xenografts are routinely used in patients (e.g., porcine dermis).[26,30–33]

Other researchers have reported successful decellularization of human-derived adipose tissue: yet, the vast majority of this research has been performed on discarded tissue collected from surgical operations.[13,15,25,27] This research has been critical to understand the biological properties of human-derived decellularized adipose tissue, but it cannot support transition to a production-scale therapy readily available for patient care. Instead, the development of an Allograft Adipose Matrix (AAM) derived from cadaveric donor tissues using a standardized and controlled method might offer the possibility for large-scale manufacturing of an off-the-shelf scaffold. The development of human cadaver-derived acellular scaffolds from other tissues (e.g., skin) has previously shown the high value of this approach.[34,35] To our knowledge, our AAM is the first human-derived, decellularized, adipose scaffold obtained from cadaveric tissue using a scalable procedure and ready to be directly applied to patients in clinical care for adipose tissue reconstruction and regeneration (Appendix Fig. A1).

In this study, we hypothesize that a shelf-ready (HCT/P product), injectable AAM obtained from human cadaveric tissue can be used for soft tissue reconstruction *in vivo* and optimize it in a preclinical murine model in preparation for subsequent translational application to patient care. We tested the *in vivo* behavior of the following:

1. (Study 1) different configurations of the AAM (small-size scaffold vs. large-size scaffold), postulating that a small-size scaffold would better support cell migration (e.g., angiogenesis and adipogenesis) within the scaffold;
2. (Study 2) the AAM grafted alone or in combination with mechanical preconditioning of the recipient site with external volume expansion (EVE), postulating that EVE would facilitate ingrowth of blood vessels within the AAM graft; and
3. (Study 3) the AAM grafted in different densities in combination with other adipose tissue, postulating that a lower density of AAM would best promote cell migration and AAM recellularization, affecting graft survival.

Overall, our hypothesis is that the AAM in combination with other treatments can best assist recipient site preparation before grafting and improve graft survival. By doing so, we aim to inform and guide clinical application of a novel off-the-shelf AAM to support autologous adipose tissue grafting in soft tissue reconstruction, allowing more effective, less invasive, and less extensive treatments.

Methods

Animal studies design

Animals were used under an approved animal protocol, and in accordance with our Institutional Animal Care and Use Committee guidelines, the ARRIVE guidelines, and the National Institutes of Health guide for the care and use of Laboratory animals. In this study, we chose to use female animals as this gender best replicates the most common clinical scenario in which adipose tissue grafting is used (in both reconstructive and aesthetic surgeries).

Study 1: *In vivo* optimization of AAM preparation/configuration. A first study was conducted on a total of 28 immunocompetent 8-week-old wild-type (strain C57BL/6) female mice (The Jackson Laboratory, Bar Harbor, ME), weighting $\sim$20 g each. Mice were procured from the same vendor, housed individually, and randomly allocated (not processed in batch, to avoid batch-related variability) to two experimental groups ($n=14$ per group) undergoing subcutaneous injection of either the small AAM or the large AAM. Animals were followed up for 1 week ($n=2$), 2 weeks ($n=2$), and 4 weeks ($n=10$) before collecting samples of the graft and control areas for analysis (Supplementary Fig. S1a; Supplementary Data are available online at www.liebertpub.com/tea).

Study 2: *In vivo* optimization of the EVE preconditioning and AAM injection combined treatment. Subsequently, an additional 66 animals (same strain, age, and sex as first set of experiments) were assigned to three experimental groups ($n=22$ per group) undergoing for 5 days continuous EVE stimulation, cyclical (moderate-intensity intermittent) EVE stimulation, or no stimulation (control). Given the small size of the mice and the possibility that EVE stimulation could have affected also the contralateral side, we opted to have a separate group as control (instead of contralateral grafting or the AAM without EVE stimulation). Five days after the last EVE stimulation, animals underwent subcutaneous injection of small AAM in the same area that was previously stimulated by EVE.

We decided to test only the small AAM since no significant biological differences between this and the large AAM were observed in the first study and the small AAM could provide easier manipulation and processing before injection. Follow-up extended to 4 weeks ($n=4$ per group), 6 weeks ($n=8$ per group), and 12 weeks ($n=10$ per group) before collecting samples of the graft and control areas for analysis (Supplementary Fig. S1b).

Study 3: *In vivo* optimization of the AAM and adipose tissue combined injection treatment. Finally, in a third experiment, a total of 15 immune-deficient (athymic nude) 8-week-old wild-type (strain nu/nu 002019; The Jackson Laboratory) female mice, weighting $\sim$20 g each, were randomly allocated (not processed in batch, to avoid batch-related variability) to three experimental groups ($n=5$ per group), each receiving a combined graft of AAM and adipose tissue in different densities as better described hereunder (AAM high density, AAM intermediate density, and AAM low density).

As we grafted human tissue, which is immunogenic, an immune-deficient model was required, even though results obtained in immunocompetent mice for Study 1 and Study 2 might not have completely replicated those observed in this model with regard to the degree of inflammation, angiogenesis, and fat necrosis or resorption. In each group, animals underwent subcutaneous injection on their left dorsum of 0.5 cc of the mixed small AAM-Lipoaspirate in one of the densities described hereunder; 0.5 cc of lipoaspirate was injected on the right dorsum to serve as control. Animals were followed up to 6 weeks before collecting samples of the graft and control areas for analysis (Supplementary Fig. S1c).

AAM preparation

AAM was provided by the Musculoskeletal Transplant Foundation (Edison, NJ) and obtained from human adipose tissue of cadaveric donors. Procurement of donor tissue was performed in accordance with existing regulations and under approved protocols. Donor tissue was screened for presence of any pathogens through serological testing and incoming bioburden identification. Adipose tissue was procured from the subcutaneous layer of full-thickness skin donors by separating, mechanically reducing, and centrifuging to isolate the adipose fraction. For each experiment, samples were derived from a single donor and a single, homogenous, batch of processed AAM.

The AAM was processed by a single investigator in a standardized manner and in an aseptic environment with ISO class 10 cleanrooms. The processing steps included the use of an organic solvent to remove the lipid component and a surfactant/ethanol-based solution to remove the cellular content and debris, while preserving the integrity of the ECM. The AAM was then disinfected with a peracetic acid- and ethanol-based solution to ensure tissue safety. Finally, the AAM was lyophilized and processed (minced and milled) to obtain an injectable AAM powder in two scaffold-size configurations, either small-size scaffold (small AAM, $\sim$100–200 μm^2) or large-size scaffold (large AAM, $\sim$1000–2000 μm^2). Other than mincing/milling, there were no other differences in the processing of the small-size and large-size AAM.

After sample preparation, tissue sterility was verified using the USP <71> Sterility Test (Nelson Labs, Salt Lake City, UT). The effectiveness of the decellularization step (threshold: <18 ng/mg of dry AAM) had been verified by quantifying the residual DNA using the Quant-iT PicoGreen dsDNA Assay Kit (Invitrogen, Carlsbad, CA). The AAM in powder form was packaged in sterile 5 cc luer-lock syringes, ready for rehydration with sterile saline solution. Further information regarding the processing of the materials are proprietary. This product falls into the HCT/P category and is ''shelf-ready'': a version of AAM similar to the one adopted in this study is currently commercially available (RENUVA®; Musculoskeletal Transplant Foundation) and has already been adopted in clinical studies.[36,37]

Lipoaspirate preparation

Lipoaspirate was obtained through manual liposuction from discarded tissue following a human panniculectomy and processed according to the established Coleman's technique.[1,2] Since the tissue had already been surgically removed, no anesthetic, tumescent solution, or other local agent was used to infiltrate the tissue. Human tissue was procured under a protocol approved by our Institutional Review Board, in accordance with existing regulations. The tissue was transferred from the operating room to the laboratory in a sterile container with ice, without any other medium. Tissue was processed and injected in animals within $\sim$40 min of its surgical procurement (Supplementary Table S1).

EVE stimulation model

A custom dome-shaped rubber device was attached on the dorsum of animals, and connected to a suction pump (ActiVAC; Kinetic Concepts, Inc., San Antonio, TX) at a pressure of −25 mmHg as previously described.[9,11,38–40] Continuous stimulation was applied for 5 days. Cyclical (moderate-intensity intermittent) EVE was administered with 0.5-h long stimulations six times per day, each separated by 1-h intervals for 5 days, based on our previously optimized protocols.[11,40] These protocols optimized the pressure, kinetic, and duration of treatment, and had shown that a 5-day follow-up after EVE is sufficient to promote angiogenesis in tissues.[11,40]

Subcutaneous injection model in immune-competent mice

The AAM powder was reconstituted with sterile saline solution to obtain a 25% rehydration ratio (mass protein-to-volume saline ratio) before *in vivo* injection; 0.5 cc of AAM was injected on the lateral left dorsum of animals using a ''tunnel technique'' and a 16-gauge blunt lipoinjection cannula.[41] Briefly, the cannula was inserted subcutaneously using a 3-mm surgical access, caudally in proximity of the root of the tail, and pushed laterally until the flank region. The graft was gradually placed subcutaneously, while retracting the cannula for 2 cm. Depending on the phase of the study and the experimental group, the procedure was either performed on one flank only or on both, bilaterally. The cannula was then removed and the surgical access was sutured.

The choice of the cannula was determined by preliminary *ex vivo* tests.

AAM + lipoaspirate subcutaneous injection model in athymic mice

The small AAM-dehydrated scaffold was reconstituted with sterile saline solution to obtain a 25% (AAM high density), 12.5% (AAM intermediate density), or 6.25% (AAM low density) rehydration ratio (protein mass to saline volume ratio) before *in vivo* injection.

The rehydrated AAM was then mixed in equal parts (50% ratio, based on mass weight) with processed lipoaspirate (Supplementary Fig. S2); 0.5 cc of the mixed AAM lipoaspirate (in different densities for each experimental group) was injected on the left dorsum of the animal, using the ''tunnel technique'' previously described. One hundred percent lipoaspirate (representative of current standard of care) was injected on the contralateral side of the dorsum

using the same procedure. There were no significant differences in preimplantation weights of grafts.

AAM + lipoaspirate in vitro *survival assay*

Staining with trypan blue was used to count the number of necrotic cells, using a standard hemocytometer and an optical microscope at 100× magnification (Nikon Coolpix S4; Nikon Corp., Tokyo, Japan), as previously described.[42] All samples were incubated for 30 min at 37°C and the rate (%) of necrotic cells (10 views) was counted by three independent investigators (the same field was counted by each investigator before moving to a different field). Cell survival was defined as the inverse of the necrotic cell rate (100% – necrotic cells % = viable cells %).

Macroscopic analysis

Qualitative analysis of the external and internal macroscopic appearance of grafts was done with digital imaging captured on the day of sample harvesting (Nikon Coolpix S4; Nikon Corp.).

After grafts were procured in a standardized technique (3 × 3 cm full-thickness biopsy, including the graft and surrounding skin), the weight (grams) of grafts was measured (using a precision scale). We did not dissect the grafts from surrounding skin and opted for larger skin biopsies because we wanted to retain the tissue surrounding the graft and process it ''*en bloc*'' for histological analysis. As we assumed that the remaining skin tissue weighted the same in all animals, we attributed the differences in weight of the biopsies to the weight of the graft. Size/volume of grafts was measured indirectly using histology as described hereunder.

Microscopic analysis

Histology [hematoxylin and eosin (H&S) staining] was used to measure the thickness and cross-sectional area of the grafts. The Aperio System (Leica Biosystems, Nussloch, Germany) was used for full-size slide scanning and the ImageJ Software (NIH, Bethesda, MD) was used for image analysis. Qualitative analysis of the ECM structure (ECM homogeneity, tissue fragmentation, etc.) of grafts was performed by an experienced investigator blinded to the group. Possible artifacts caused by histological processing were considered in this evaluation. The cross-sectional area of histological sections of the grafts was used as a surrogate method to assess graft volume/retention over time. Graft cross-sections were obtained by cutting the central portion of each sample; cross-sectional area was digitally measured using the ImageJ Software (NIH) on previously scanned slides. This information is different from what was obtained from the weight of grafts, but complements it and provides a separate, additional analysis of graft survival/retention.

Immunohistochemistry was used to quantify graft and perigraft angiogenesis using an endothelial cell marker platelet endothelial cell adhesion molecule-1 (CD31). Instead, to qualitatively analyze graft/perigraft adipocyte proliferation/infiltration, we used the lipid droplet surface marker Perilipin A. Images of the microscopy slides were acquired at a standard magnification (10x) using a Nikon E200 Microscope (Nikon Corp.) and quantified using the ImageJ Software (NIH).

Quantification of blood vessel density was performed according to previously described and validated methods.[9,11,40,43] Briefly, three random images at standard magnification (10×) of $CD31^+$ histological sections were acquired as previously described and blood vessels were manually counted using the ''Cell Count'' extension of the ImageJ Software. Capillary density was expressed as the average number of $CD31^+$ vessels per magnification field.

Perilipin A is an established marker for assessing adipocyte proliferation and graft infiltration.[39,40,44–46]

Data and statistical analysis

Animals were procured from the same vendor, housed individually, and randomly allocated (not processed in batch, to avoid batch-related variability) to groups; samples were randomly processed. Investigators in charge of data collection and analysis were blinded to treatment. Sample size was calculated to detect meaningful differences (α: 0.05; power: 95%) between treated and control groups with regard to the primary endpoint (angiogenesis). Secondary endpoints included an increase in AAM grafts cross-sectional area and weight compared to controls.

Based on our preliminary experience on regenerative scaffolds, we postulated that the effects of the treatments (AAM alone, in combination with EVE, or combined to adipose tissue) would have increased graft angiogenesis by 60% or more (anticipated effect for controls: 18 ± 5 blood vessels per magnification field) at follow-up: to show statistical significance, a $n = 5$ per group was then required. All data were analyzed by three researchers blinded to the treatment. Differences between groups were quantified and expressed as a mean ± standard deviation (SD). The significance of differences was evaluated with analysis of variance and Bonferroni *post hoc* correction. A p-value <0.05 was considered statistically significant.

Results

Study 1: In vivo *optimization of the AAM configuration*

AAM configuration does not affect volume retention over time. In both AAM configurations (small AAM and large AAM), the AAM graft was evident in tissues at a 2- and 4-week follow-up. No significant difference was observed in the external and internal (after dissection) macroscopic appearance of the grafts between the two groups (Supplementary Fig. S3).

Consistently, histology revealed no significant difference in volume retention between groups at all time points (weeks 1, 2, and 4). In the small AAM group, a 1.4-fold ±0.2 increase in cross-sectional area was observed over time (week 4 vs. week 1, $p < 0.05$). Measurement of graft cross-sectional area on histological sections was used as a surrogate marker to assess graft volume retention, assuming a consistent behavior of the grafts along their entire length and among groups. Consistently, at qualitative histological analysis performed by an experienced investigator blinded to the group, the ECM architecture appeared better preserved in the small AAM group (Supplementary Table S2).

The AAM robustly stimulates perigraft angiogenesis possibly through an inflammation-mediated mechanism. Both AAM configurations showed a higher angiogenic response

in tissues surrounding the grafts (1.5-fold ±0.2 increase on week 4 compared to controls, $p < 0.05$). No significant differences were observed between the two configurations at any time point. The increased vascular density was already present at a 1-week follow-up, peaked at a 2-week follow-up, and later (week 4) decreased to the same values as of early assessments (Fig. 1, Supplementary Table S2).

At weeks 1 and 2, the AAM grafts were surrounded by an intense inflammatory reaction (observed at histology as a thick perigraft accumulation of inflammatory cells creating), which increased by week 4. The large AAM configuration generated a thicker inflammatory infiltrate (qualitative analysis, differences were not measured) (Supplementary Fig. S4). Yet, observed differences in local inflammatory response between small AAM and large AAM grafts seemed to not cause significant differences in perigraft angiogenesis.

Summary of results from Study 1. Both small AAM and large AAM grafts retained volume over time and similarly promoted angiogenesis in surrounding recipient tissues. Large AAM grafts seem to elicit a more intense inflammatory reaction in a nonimmune-deficient xenogenic model; no other significant biological differences were noted between the two preparations.

Study 2: In vivo *optimization of EVE preconditioning and AAM combination treatment*

EVE preconditioning shows long-term vascularization of small AAM grafts. Density of capillaries surrounding and invading the small AAM grafts after preconditioning with cyclical (moderate-intensity intermittent) EVE showed a 1.6-fold ±0.2 increase at a 12-week follow-up compared to

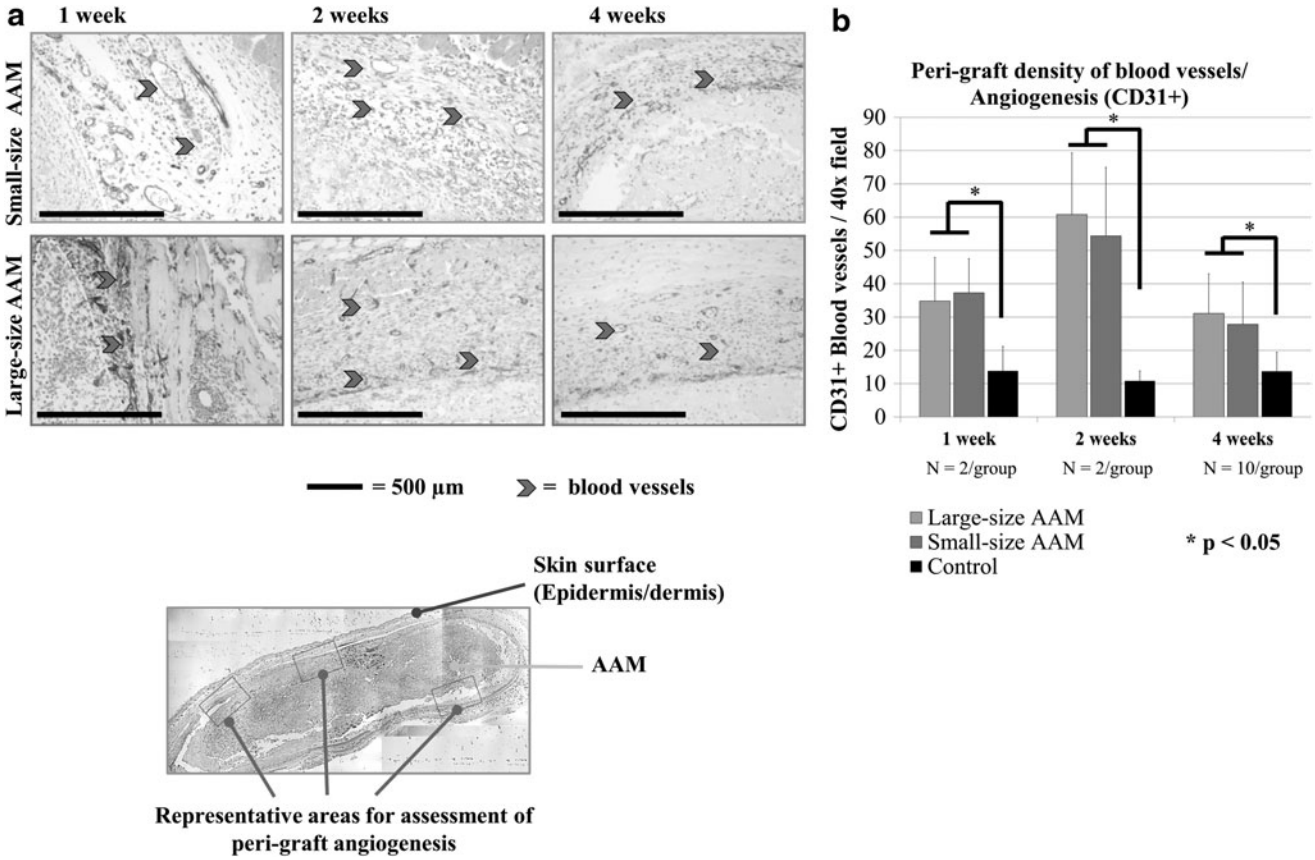

FIG. 1. Angiogenic effect of small AAM and large AAM. This panel shows angiogenesis in the tissue surrounding the grafts as assessed by immune histochemistry for the endothelial marker CD31. As angiogenesis is a key component of graft recellularization and survival, we assessed how different configurations of the AAM (small AAM and large AAM) would have affected it. The two scaffold-size configurations uniquely differ for the mincing of their ECM particles (small AAM, $\sim$100–200 µm^2, or large AAM, $\sim$1000–2000 µm^2). Our results show that both small AAM and large AAM promote perigraft angiogenesis compared to controls; no significant differences were observed between the two configurations. **(a)** CD31 staining (in *brown*, highlighted by *red arrows*) for blood vessels shows endothelial cells sprouting within the AAM grafts from their borders starting from week 1 in all groups. In figure below at smaller magnification is provided as reference of tissue orientation. The area marked in *yellow* represents the AAM graft. Magnification: 40×; reference bar = 500 µm. **(b)** Outcomes of measurements on histological images. Quantification of blood vessel density was performed according to previously described and validated methods.[9,11,40,43] Briefly, three random images at standard magnification (10×) of CD31$^+$ histological sections were acquired as previously described and blood vessels were manually counted using the ''Cell Count'' extension of the ImageJ Software. Capillary density was expressed as the average number of CD31$^+$ vessels per magnification field. One-way ANOVA with Bonferroni *post hoc* correction. A value of $p < 0.05$ was considered statistically significant. Data are expressed as CD31$^+$ blood vessels per 40× magnification field. AAM, Allograft Adipose Matrix; ANOVA, analysis of variance; ECM, extracellular matrix.

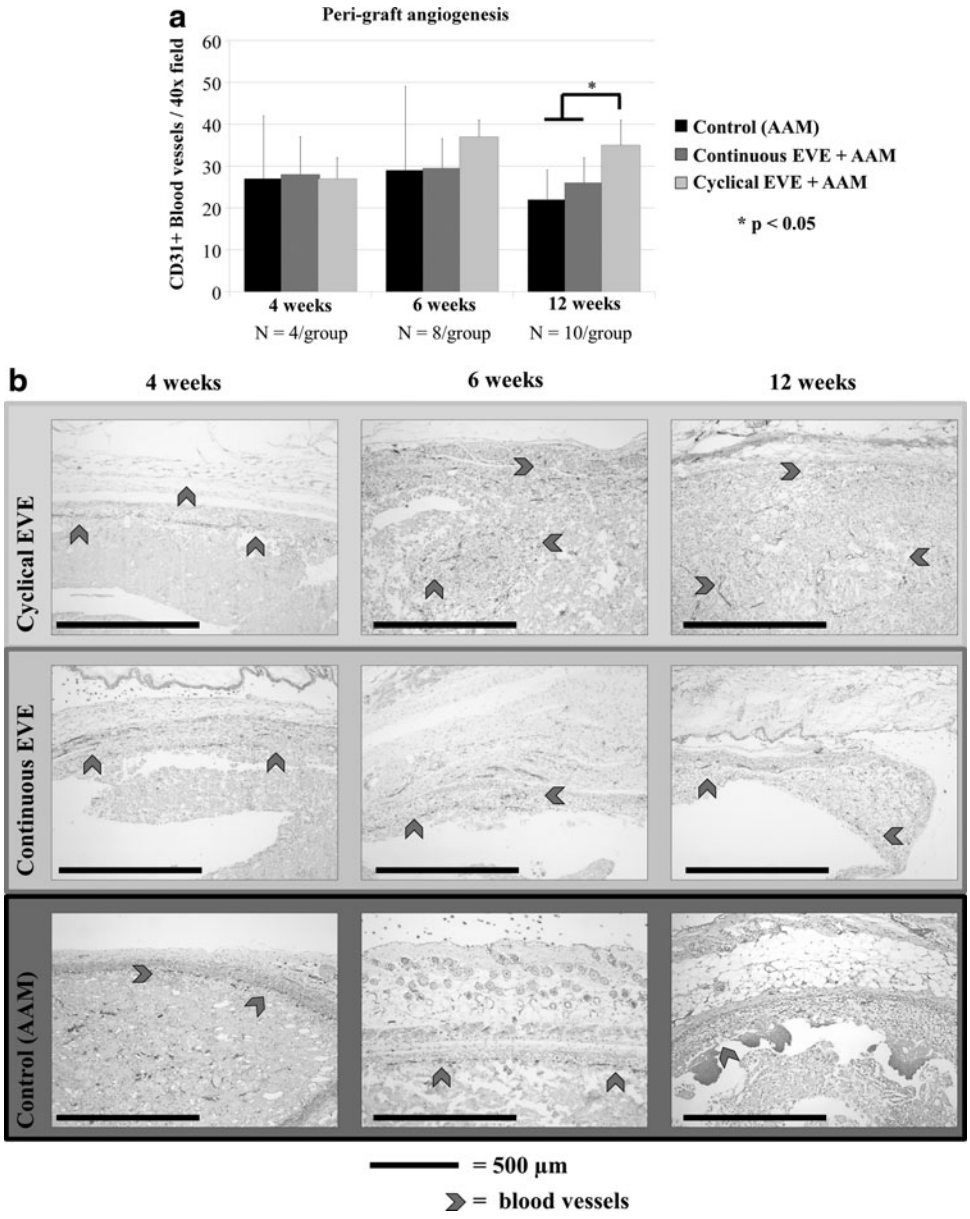

FIG. 2. Angiogenic effect of EVE and AAM. This panel shows angiogenesis in the tissue surrounding the grafts as assessed by immune histochemistry for the endothelial marker CD31. As angiogenesis is a key component of graft recellularization and survival, we assessed how different combinations of EVE and the AAM would have affected it. EVE is a technique for improving vascularity of tissues by applying external suction on skin, under a controlled protocol. EVE was performed according to a previously established and optimized protocol or in a continuous mode.[40] Our results show cyclical EVE promotes the highest perigraft angiogenesis at a long-term follow-up, compared to controls or continuous stimulation. No significant differences were observed at earlier time point, possibly due to the need for a longer assessment on the survival and remodeling of grafted tissue. **(a)** Outcomes of measurements on histological images. Quantification of blood vessel density was performed according to previously described and validated methods.[9,11,40,43] Briefly, three random images at standard magnification (10×) of $CD31^+$ histological sections were acquired as previously described and blood vessels were manually counted using the ''Cell Count'' extension of the ImageJ Software. Capillary density was expressed as the average number of $CD31^+$ vessels per magnification field. One-way ANOVA with Bonferroni *post hoc* correction. A value of $p < 0.05$ was considered statistically significant. Data are expressed as $CD31^+$ blood vessels per 40× magnification field. **(b)** CD31 staining (in *brown*, highlighted by *red arrows*) for blood vessels shows endothelial cells sprouting within the AAM grafts starting from week 4 in all groups. Magnification: 40×; reference bar = 500 µm. EVE, external volume expansion.

control ($p < 0.05$) (Fig. 2a, b, Supplementary Table S3). This difference was already noted at earlier time points (6-week follow-up), but was not statistically significant due to the high intragroup variability of controls; no other significant differences were noticed among groups at earlier time points. Continuous EVE did not significantly induce angiogenesis compared to controls. Histology provided clear visual confirmation of the increased graft vascularity in the cyclical EVE group. Immunohistochemistry clearly showed how the angiogenic process occurred at the periphery of

grafts at earlier time points and gradually infiltrated the inner core of grafts at later time points (Fig. 1a).

A robust inflammatory response was observed along the peripheral border of the grafts in all groups. Both cyclical and continuous EVE led to a 1.3-fold ±0.3 increase in thickness of the inflammatory infiltrate surrounding the small AAM grafts compared to controls ($p < 0.05$) at early time points (4-week follow-up), but this difference was not present at longer follow-ups (Supplementary Fig. S5a, b, Supplementary Table S3).

EVE preconditioning does not increase long-term retention of small AAM grafts. Macroscopic and histological analysis of small AAM grafts showed gradual reabsorption (weight and cross-sectional area) over time and loss of intragraft ECM architecture for all groups (Figs. 3 and 4, Supplementary Fig. S6, Supplementary Table S3). Preconditioning with cyclical EVE significantly increased the weight of the grafts at a 4-week follow-up, but no difference was noted at subsequent time points (Fig. 3, Supplementary Table S3).

Histological analysis of grafts that were preconditioned with cyclical EVE showed a better-preserved ECM architecture, and graft structure with less areas of fragmented matrix or vacuoles, compared to continuous EVE (Fig. 4b, Supplementary Table S3).

Adipogenesis occurs at the periphery of the small AAM. Histological analysis revealed clusters of adipocytes at the periphery of the small AAM grafts, along the external border next to the areas of inflammatory infiltrate. Adipocytes stained with Perilipin A could be observed starting from a 4-week follow-up in all groups, with larger and more frequent clusters in groups that had received preconditioning with cyclical or continuous EVE compared to controls (Fig. 5). Given the scattered distribution of adipocyte clusters over the tissue, it was not possible to perform a quantitative analysis of this process or monitor it over time.

Summary of results from Study 2. Small AAM undergoes recellularization by adipogenesis, starting at the graft margins. Combination of AAM grafts with cyclical EVE enhances long-term perigraft angiogenesis; this effect is not sufficient to increase graft survival, but might contribute to an improvement in the structural quality of grafts.

Study 3: In vivo *optimization of small AAM and adipose tissue combination treatment*

Varying densities of small AAM combined with adipose tissue do not affect adipocyte viability *in vitro*. *In vitro* testing of different combinations of small AAM and adipose tissue (human lipoaspirate) showed that the low-density AAM led to a higher cell viability (96.7% ± 2.3) compared to the intermediate-density AAM (86.0% ± 5.9) and the high-density AAM (85.4% ± 3.5), although no statistically significant differences were observed. All groups performed similarly to lipoaspirate alone (95.5% cell viability) or lipoaspirate mixed with saline solution (50% ratio) (95.3% cell viability) (Supplementary Fig. S7).

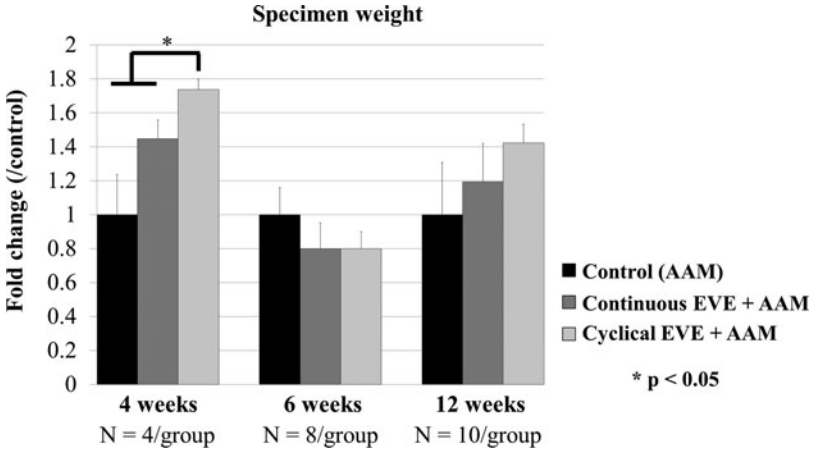

FIG. 3. Measurement of survival of AAM grafts with/without preconditioning with EVE. This panel shows the assessment of graft weights after sample procurement, as a surrogate method to assess graft survival. EVE is a technique for improving vascularity of tissues by applying external suction on skin, under a controlled protocol. As we hypothesized that combination of EVE and AAM grafts would have enhanced grafts' survival, we tested how different protocols or EVE (or no EVE) affected AAM grafts *in vivo*. EVE was performed according to a previously established and optimized protocol or in a continuous mode.[40] Grafts and control areas were procured using a standardized technique (3 × 3 cm full-thickness biopsy, including the graft and surrounding skin), and the weight (grams) of grafts was measured using a precision scale. We did not dissect the grafts from surrounding skin and opted for larger skin biopsies because we wanted to retain the tissue surrounding the graft and process it ''*en bloc*'' for histological analysis. As we assumed that the remaining skin tissue weighted the same in all animals, we attributed the differences in weight of the biopsies to the weight of the graft. No significant differences were observed among groups at long-term follow-up. The short-term increase in graft weight at 4-week follow-up could relate to the presence of EVE-induced edema within the grafts, as suggested by the parallel increase in tissue inflammation. This difference was statistically significant for cyclical EVE versus both continuous EVE and controls. Weight persistence immediately after en bloc excision of a 3 × 3 cm standardized biopsy. One-way ANOVA with Bonferroni *post hoc* correction. A value of $p < 0.05$ was considered statistically significant. Data are expressed as the fold change over control ± SD. SD, standard deviation.

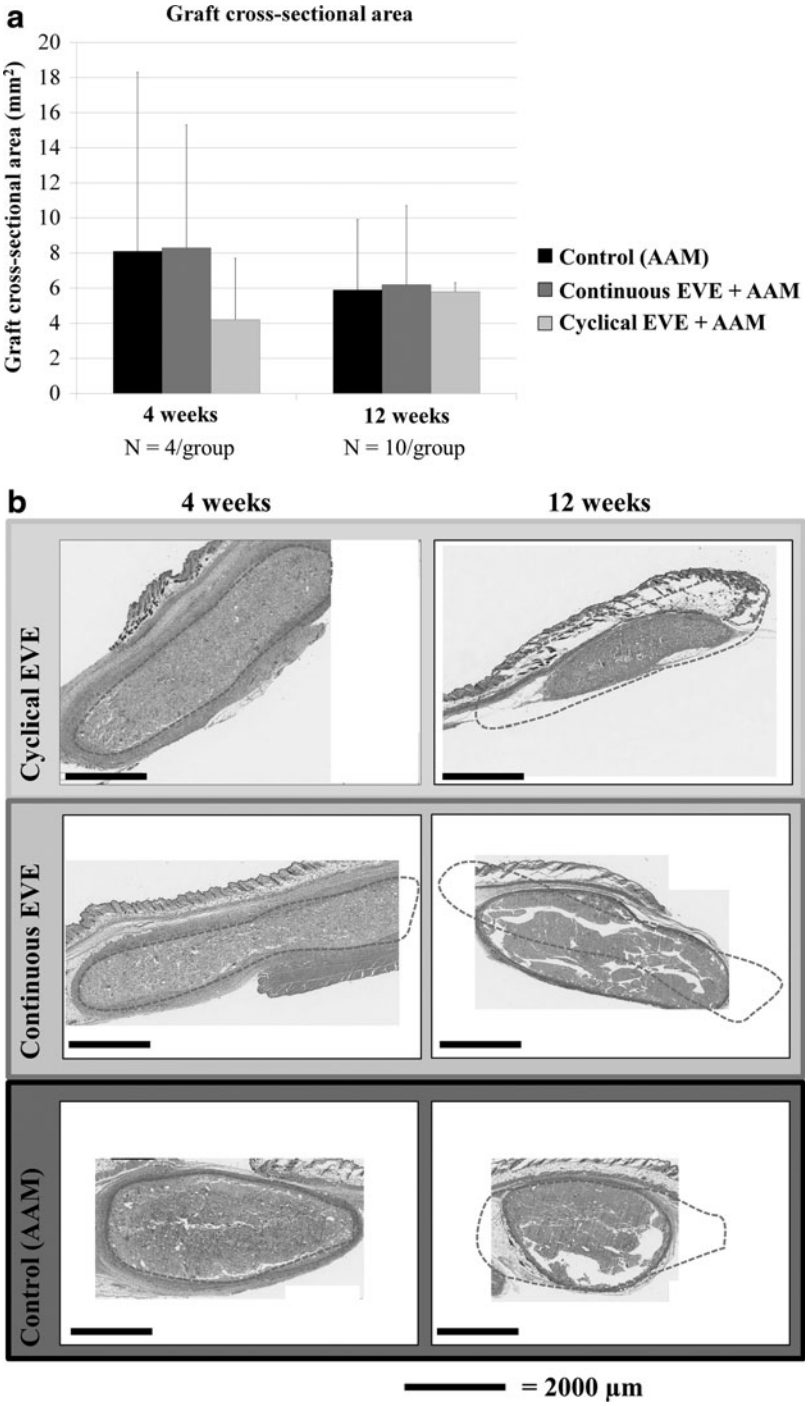

FIG. 4. Measurement of volume retention of AAM grafts with/without preconditioning with EVE. This panel shows the assessment of the cross-sectional area of grafts measured on H&E-stained histological sections. This assessment was used as a surrogate method to assess graft survival and volume retention. Graft cross-sections were obtained by cutting the central portion of each sample; cross-sectional area was digitally measured using the ImageJ Software (NIH, Bethesda, MD) on previously scanned slides. This information is different from what was obtained from the weight of grafts, but complements it and provides a separate, additional analysis of graft survival/retention. Our results show that no significant differences were observed among groups at all time points. Differences with outcomes observed in samples' weights might relate to the loss of tissue fluids (e.g., edema) during processing of histological sections so that the group with the highest weight resulted in the lowest cross-sectional area (highest loss of fluid-related weight). **(a)** Cross-sectional area of AAM grafts measured with histology on microscopic samples. One-way ANOVA with Bonferroni *post hoc* correction. A value of $p < 0.05$ was considered statistically significant. Data are expressed as the fold change over control ± SD. **(b)** H&E staining shows gradual AAM reabsorption over time and increasing fragmentation of its internal ECM at 12-week follow-up in the continuous EVE group and the control group. The *red dotted lines* highlight the cross-sectional area of the graft at the 4-week follow-up, whereas the *green dotted lines* highlight the cross-sectional area of the graft at the 12-week follow-up. Despite images at different time points not belonging to the same grafts and uniquely representing the behavior of grafts in each group, we overlaid the *red dotted lines* in the *left column* to show gradual reduction of graft cross-sectional area, representative of graft reabsorption, over time. Magnification: 4×; reference bar = 2000 µm. H&E, hematoxylin and eosin.

Varying densities of combined small AAM and adipose tissue do not affect graft weight or retention. No significant differences were observed in the graft morphology at macroscopic qualitative analysis (visual inspection of the appearance of the grafts before/after surgical dissection) among the three groups and between the three groups and controls (Supplementary Fig. S8).

Analysis of weight of grafts showed that the high-density AAM had a statistically significant difference in weight (1 ± 0.2 g vs. 0.5 ± 0.1 g, $p < 0.05$) compared to its internal control (adipose tissue only) (Supplementary Fig. S8, Supplementary Table S4). Despite assessing a different aspect of graft retention (weight vs. cross-sectional area), histological analysis of the cross-sectional area of the grafts confirmed this finding by showing a higher cross-sectional area in the high-density AAM group. Yet, no statistical significance was achieved likely due to the high intragroup variability (SD) of the high-density AAM. No significant differences in the graft cross-sectional area were noted between the other experimental groups (intermediate-density AAM and low-density AAM) and controls at histological analysis (Supplementary Fig. S9, Supplementary Table S4).

At qualitative analysis of specimens, the low-density AAM showed a better-preserved architecture with less cystic-like areas (Fig. 6).

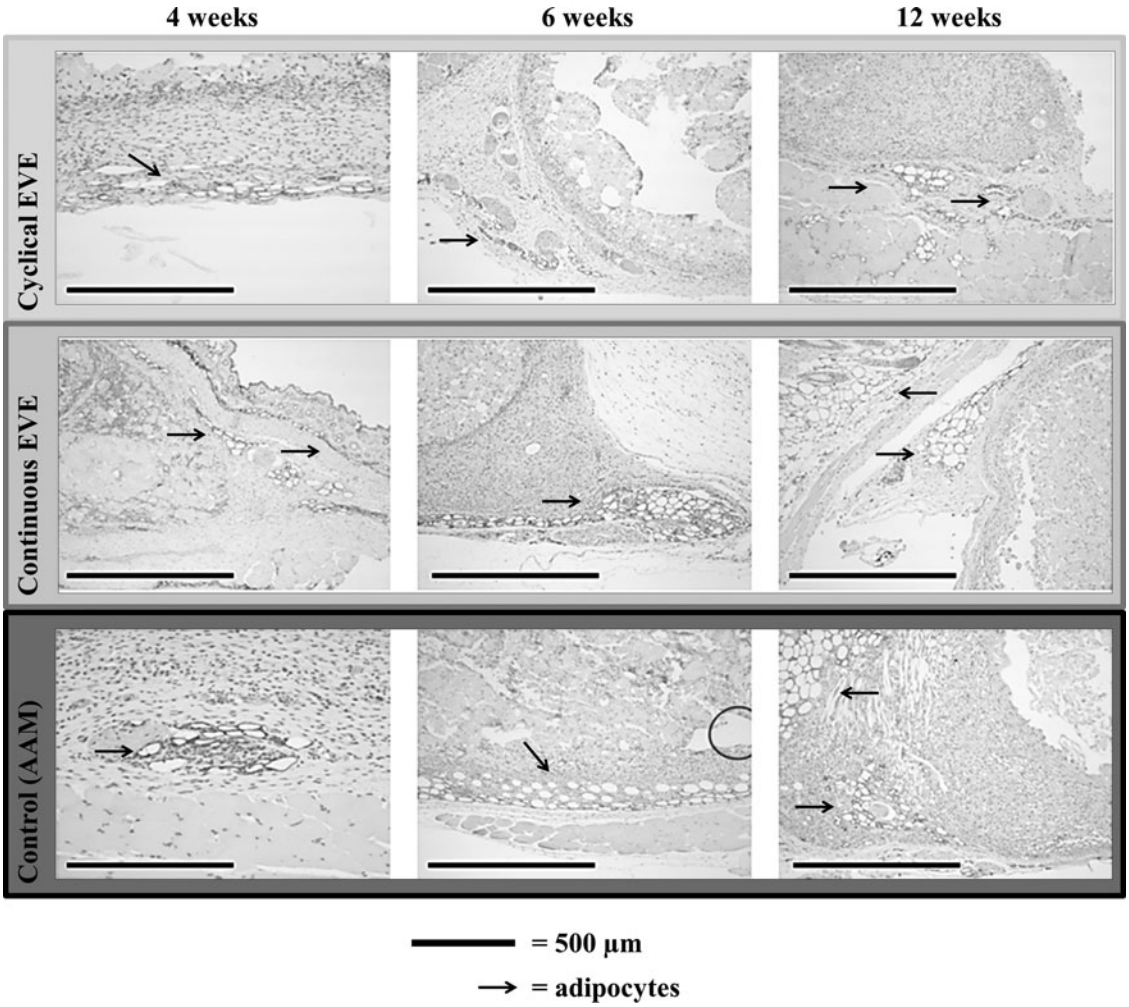

FIG. 5. Adipogenic effect of EVE and AAM. This panel shows adipogenesis in the tissue surrounding the grafts as assessed by immune histochemistry for the adipocyte marker Perilipin A. As adipogenesis is a key component of graft recellularization and decellularized adipose scaffold has shown the ability to induce adipogenesis, we assessed how different combinations of EVE and the AAM would have affected it. EVE is a technique for improving vascularity of tissues by applying external suction on skin, under a controlled protocol. Previous studies have also shown that EVE can promote adipogenesis.[11,39] EVE was performed according to a previously established and optimized protocol or in a continuous mode.[40] Perilipin A is an established marker for assessing adipocyte proliferation and graft infiltration.[39,40,44–46] Images show clusters of adipocytes at the periphery of the AAM grafts, along the external border next to the areas of inflammatory infiltrate. Adipocytes stained with Perilipin A could be observed starting from a 4-week follow-up in all groups, with larger and more frequent clusters in groups that had received preconditioning with cyclical or continuous EVE compared to controls. Yet, given the scattered distribution of adipocyte clusters over the tissue, it was not possible to perform a quantitative analysis of this process. Perilipin A staining (in *brown*, highlighted by *black arrows*) for adipocytes shows infiltrating clusters of adipogenic proliferation at the periphery of the AAM grafts starting from week 4 in all groups. Magnification: 40×; reference bar = 500 μm.

Combined small AAM and adipose tissue grafts promote angiogenesis similar to adipose tissue grafts; combination of low-density AAM and adipose tissue shows higher angiogenesis. Histological analysis with immunohistochemistry revealed comparable density of blood vessels surrounding and infiltrating the AAM and adipose tissue grafts and control grafts (adipose tissue). Low-density AAM and adipose tissue grafts were characterized by a significantly increased angiogenesis (1.5-fold increase, 27.8 ± 11.6 vs. 21.3 ± 6.7 blood vessels per magnification field) compared to its internal control (Fig. 7, Supplementary Table S4). Qualitative analysis demonstrated no relevant differences among groups with regard to the distribution of vessels (along the graft borders) (Fig. 7).

Combined small AAM and adipose tissue grafts enable adipocyte survival and promote adipogenesis; combination of low-density AAM and adipose tissue shows higher adipogenesis. Immunohistochemical staining with Perilipin A revealed widespread clusters of viable adipocytes in all groups (Fig. 8). Adipocytes were observed at the periphery of the grafts as well as in their inner cores. Both the low-density AAM and adipose tissue grafts and the intermediate-density AAM and adipose tissue grafts showed higher and

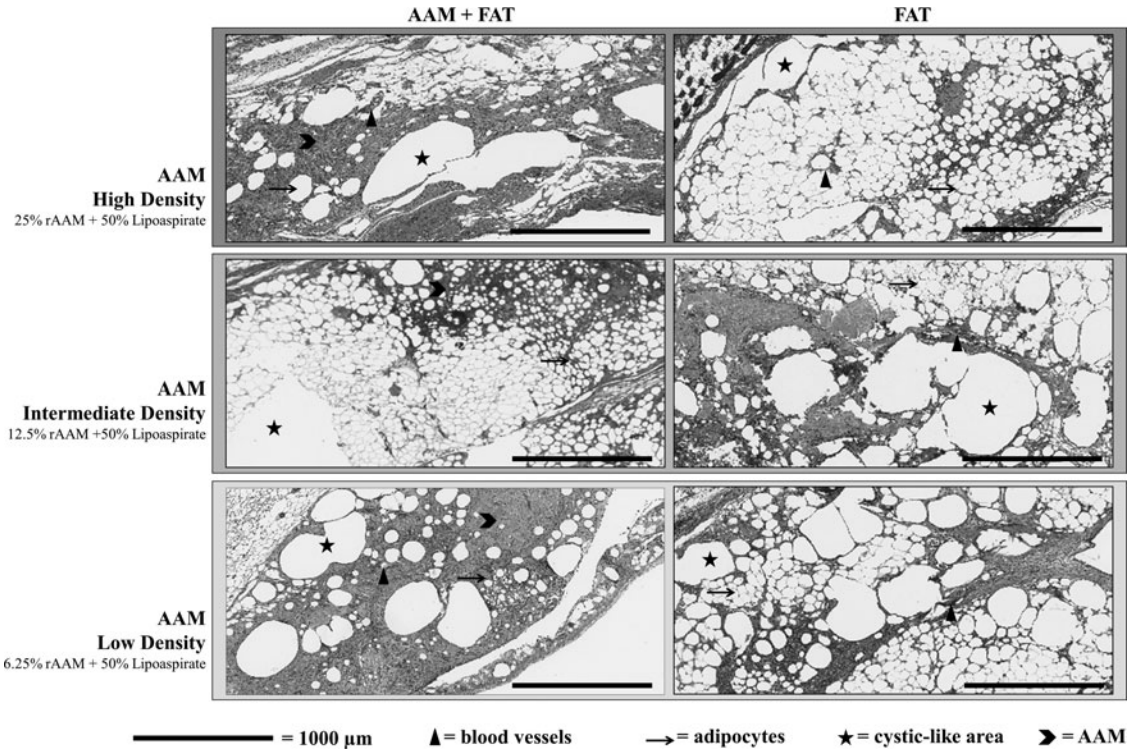

FIG. 6. Assistance of adipose tissue survival by the AAM. This panel shows the histological characteristics and biological of the combined behavior of AAM grafts combined to adipose tissue in different densities. The small AAM dehydrated scaffold was reconstituted with sterile saline solution to obtain a 25% (AAM high density), 12.5% (AAM intermediate density), or 6.25% (AAM low density) rehydration ratio (protein mass to saline volume ratio) before *in vivo* injection. The rehydrated AAM was then mixed in equal parts (50% ratio, based on mass weight) with processed lipoaspirate (Supplementary Fig. S2); 0.5 cc of the mixed AAM-lipoaspirate (in different densities for each experimental group) was injected on the left dorsum of the animal, using the ''tunnel technique'' as previously described. One hundred percent lipoaspirate (representative of current standard of care) was injected on the contralateral side of the dorsum using the same procedure. We postulated that a lower density of AAM would best promote cell migration and AAM recellularization, affecting graft survival. Qualitative analysis of the ECM structure (ECM homogeneity, tissue fragmentation, etc.) of grafts was performed by an experienced investigator blinded to the group. Possible artifacts caused by histological processing were considered in this evaluation. The *column* on the *right* represents internal controls for each group (although all similarly represent control adipose tissue—lipoaspirate). H&E staining shows viability of adipocytes in the experimental groups (rAAM + FAT, all densities) with limited areas of cystic-like necrosis and vacuoles. Low-density AAM and adipose tissue grafts demonstrate a better preservation of the graft architecture and a higher quality of graft ECM. Adipose tissue samples without AAM (FAT only) show higher rates of vacuoles, cystic-like areas of necrosis (*black asterisk*), and ECM fragmentation. Magnification: 100×; reference bar = 1000 μm. FAT, adipose tissue (lipoaspirate); rAAM, rehydrated Allograft Adipose Matrix.

more diffuse presence of adipocytes compared to other experimental groups, with adipose cells populating almost the entire graft. The experimental groups exhibited smaller adipocytes compared to controls, indicating the presence of an ongoing adipogenic process (Fig. 8).

Summary of results from Study 3. Combinations of low-density AAM and adipose tissue grafts optimize graft angiogenesis and adipogenesis, compared to combinations with other AAM densities. No differences were noted among groups with regard to the effect of AAM densities on long-term graft retention and survival.

Discussion

In the last decade, autologous adipose tissue grafting has transformed reconstructive surgery, providing a minimally invasive, safe, and biologic alternative to complex procedures or synthetic materials; yet, lack of volume retention at follow-up remains a critical limitation of the technique.[1–3,6,7,45,47–51] In our study, we hypothesize that the combined application of an injectable Allograft Adipose Matrix (AAM) and tissue preconditioning using mechanical forces (EVE) could optimize site preparation before autologous grafting, and therefore improve autologous graft survival.

Different from other decellularized scaffolds described in previous preclinical studies, the novelty of the AAM lies in the fact that it is derived from human cadavers with techniques and methods that allow its direct use on patients for surgical procedures aimed at adipose tissue reconstruction and regeneration. As previously mentioned, the AAM is categorized as HCT/P and is ''shelf-ready'': a version of AAM similar to the one adopted in this study is currently commercially available (RENUVA®; Musculoskeletal Transplant Foundation) and has already been adopted in clinical studies.[36,37]

In the first set of experiments, we have shown that both AAMs made of either small-size scaffolds and large-size

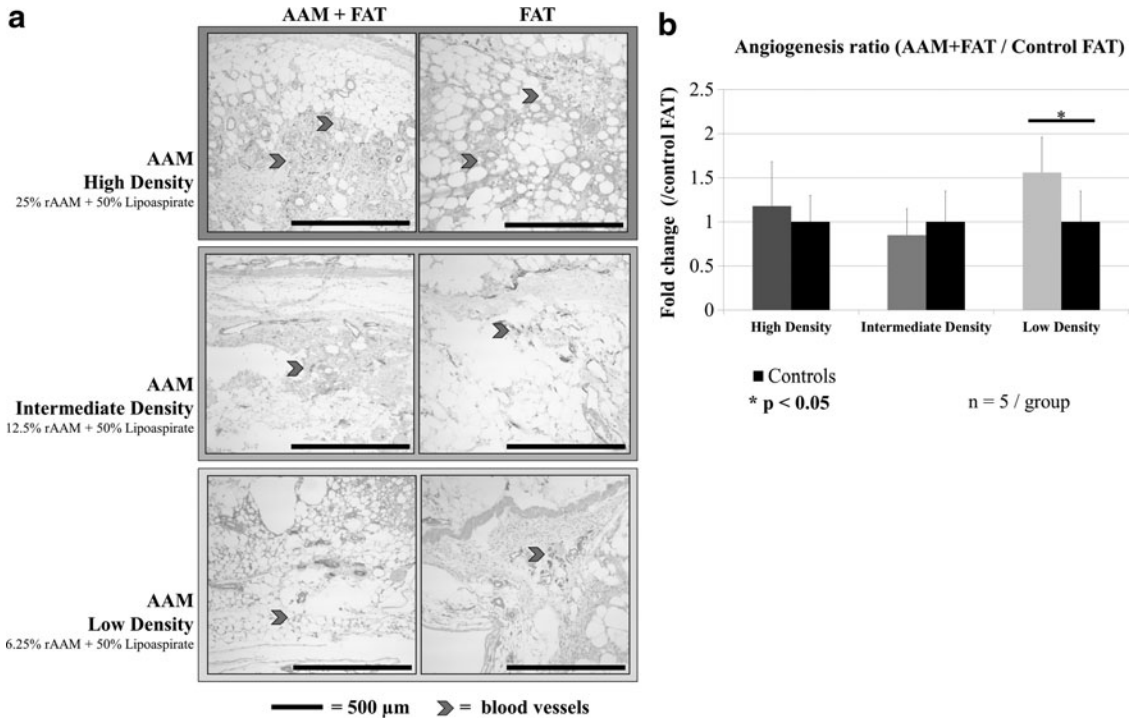

FIG. 7. Angiogenic effect of varying densities of AAM and adipose tissue grafts. This panel shows angiogenesis in the tissue surrounding the grafts as assessed by immune histochemistry for the endothelial marker CD31. As angiogenesis is a key component of graft recellularization and survival, we assessed how different combinations/densities of AAM and adipose tissue would have affected it. The small AAM dehydrated scaffold was reconstituted with sterile saline solution to obtain a 25% (AAM high density), 12.5% (AAM intermediate density), or 6.25% (AAM low density) rehydration ratio (protein mass to saline volume ratio) before *in vivo* injection. The rehydrated AAM was then mixed in equal parts (50% ratio, based on mass weight) with processed lipoaspirate (Supplementary Fig. S2); 0.5 cc of the mixed AAM-lipoaspirate (in different densities for each experimental group) was injected on the left dorsum of the animal, using the ''tunnel technique'' as previously described. One hundred percent lipoaspirate (representative of current standard of care) was injected on the contralateral side of the dorsum using the same procedure. We postulated that a lower density of AAM would best promote blood vessel migration within the AAM, including angiogenesis. Our results show that the low-density AAM had a significantly higher density of blood vessels at follow-up. **(a)** CD31 staining (in *brown*, highlighted by *red arrows*) for blood vessels shows endothelial cells infiltrating the entire AAM and adipose tissue grafts. Magnification: 40×; reference bar = 500 µm. **(b)** Outcomes of measurements on histological images. Quantification of blood vessel density was performed according to previously described and validated methods.[9,11,40,43] Briefly, three random images at standard magnification (10×) of $CD31^+$ histological sections were acquired as previously described and blood vessels were manually counted using the ''Cell Count'' extension of the ImageJ Software. Capillary density was expressed as the average number of $CD31^+$ vessels per magnification field. One-way ANOVA with Bonferroni *post hoc* correction. A value of $p < 0.05$ was considered statistically significant. Data are expressed as $CD31^+$ blood vessels per 40× magnification field.

scaffolds (a 10-fold difference in scaffold size) provided a similar graft retention over time as well as robust angiogenic stimuli to surrounding tissues (1.5-fold increase in blood vessels compared to controls). We also observed substantial peripheral inflammation surrounding the grafts and relate this finding to the use of a xenogeneic graft in an immune-competent animal model. Several studies have highlighted the interplay between localized tissue inflammation and promotion of angiogenesis, also in the context of grafted tissues and biomaterials.[52,53]

Our findings seem to confirm these phenomena, and the inflammatory reaction observed at the periphery of both the small AAM and large AAM grafts might represent one of the mechanisms of action responsible for the increased density in blood vessels measured at the periphery of the grafts. Yet, the lack of significant differences in perigraft angiogenesis between the two groups, despite an evident difference in perigraft inflammation, seems to suggest that other additional mechanisms (e.g., graft-induced angiogenesis) might have contributed to the observed angiogenic outcomes or that the inflammation-induced angiogenesis might show a plateau effect.

Inflammation has also been reported to be a major inductive factor for adipogenesis.[38,39,54] As we noted clusters of adipocytes at the periphery of AAM grafts in our study, our findings might suggest that the AAM promotes adipogenesis also through an inflammation-mediated process.[15,32,46] Yet, we were not able to perform a quantitative analysis of the adipogenic phenomenon.

This outcome suggests that the biological behavior of the AAM is independent from its configurations (size of the ECM particles of the AAM), at least in the investigated range. From a clinical perspective, however, scaffold size is relevant since it affects the viscosity of the AAM and the

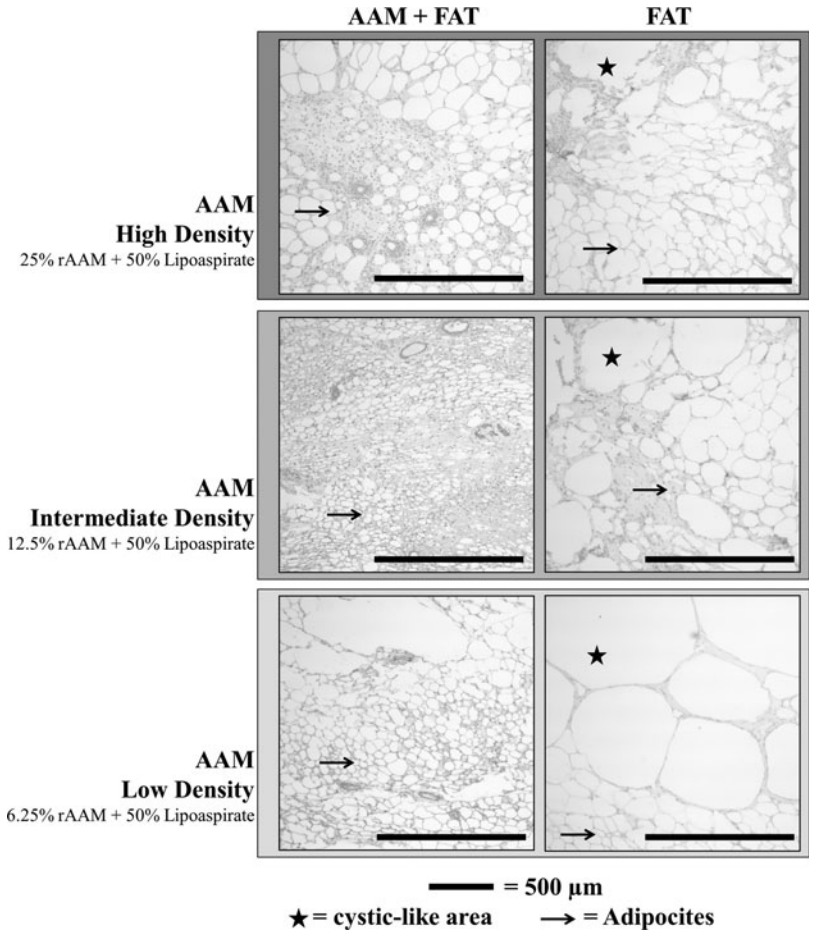

FIG. 8. Adipogenic effect of the AAM. This panel shows adipose tissue within the grafts as assessed by immune histochemistry for the adipocyte marker Perilipin A. We assessed how different combinations/densities of AAM and adipose tissue would have affected survival of grafted cells and/or recellularization (by adipogenesis) of the AAM. Perilipin A is an established marker for assessing adipocyte proliferation and graft infiltration.[39,40,44–46] The small AAM dehydrated scaffold was reconstituted with sterile saline solution to obtain a 25% (AAM high density), 12.5% (AAM intermediate density), or 6.25% (AAM low density) rehydration ratio (protein mass to saline volume ratio) before *in vivo* injection. The rehydrated AAM was then mixed in equal parts (50% ratio, based on mass weight) with processed lipoaspirate (Supplementary Fig. S2); 0.5 cc of the mixed AAM-lipoaspirate (in different densities for each experimental group) was injected on the left dorsum of the animal, using the ''tunnel technique'' as previously described. One hundred percent lipoaspirate (representative of current standard of care) was injected on the contralateral side of the dorsum using the same procedure. We postulated that a lower density of AAM would best promote recellularization and cell proliferation within the AAM. Adipocytes were observed at the periphery of the grafts as well as in their inner cores in all groups. At a qualitative evaluation performed by an expert investigator, both the low-density AAM and adipose tissue grafts and the intermediate-density AAM and adipose tissue grafts showed a higher and more diffuse presence of adipocytes compared to other experimental groups, with adipose cells populating almost the entire graft. Yet, we were not able to perform a quantitative analysis of the actual cell densities in each sample. The experimental groups exhibited smaller adipocytes compared to controls, which could indicate the presence of ongoing adipocyte proliferation. In controls, several cystic-like areas likely due to cell necrosis can be observed: cystic-like areas are present also in experimental samples, yet these should not be confused with artifacts due to histological processing (e.g., in the *top portion* of the low-density AAM and adipose tissue grafts figure). Magnification: 40×; reference bar = 500 μm.

capacity to inject it through cannulas. This hypothesis was confirmed by our *ex vivo* and *in vivo* tests in the early phases of the study, leading us to choose the easily injectable small AAM for subsequent studies. In *ex vivo* tests, the small AAM provided a better handling (preparation and injection) compared to the large AAM, a critical factor affecting the potential use by surgeons in an operating room.[47]

In the second set of experiments of our studies, we observed that the regenerative capacity of the AAM combined with cyclical EVE creates an optimized recipient environment for autologous grafts. Our results show a 1.6-fold increase in vascular infiltration in the AAM and EVE group compared to control AAM grafts, even at a long-term follow-up (12 weeks in our murine model). The impact of improved angiogenesis on the survival of adipose tissue grafts is supposed to be higher in the early phases after grafting, when grafted tissue is subjected to the highest hypoxic damage. Yet, later increments in angiogenesis might suggest

a higher tissue survival at early phases of grafting, resulting in a subsequent remodeling of tissue (including a higher vascularization).

Consistent with our previous studies, the mechanism of action of EVE seems to be linked to a transient inflammatory response.[9,11,38–40,55] The inflammation could relate to either the grafting of a xenogeneic material in an immune-competent animal model (despite the lack of cellular components in AAM that should have limited such phenomenon) or an inflammation-mediated adipogenic effect of the AAM. Yet, the higher inflammatory rate observed in EVE-treated samples at 4 weeks after treatment suggests a predominant role of EVE in driving inflammation (and possibly adipogenesis) in tissues.

Indeed, continuous application of EVE led to suboptimal outcomes, as shown by a high fragmentation of the ECM of the AAM, depicting a harmful effect on the AAM and the surrounding environment, probably due to excessive tissue inflammation temporarily persisting after the end of the EVE treatment.[9,11,38–40,55] Proliferation and maintenance of adipose tissue require an extensive network of capillaries, linking angiogenesis to adipogenesis.[6] The synergistic angiogenic and adipogenic potentials of cyclical EVE and AAM grafts suggest that their combined use creates an ideal microenvironment for survival of autologous adipose tissue grafts.

Yet, no significant differences were observed in terms of graft retention among groups, suggesting that combinations of EVE and AAM, without the addition of cellular components (e.g., adipose tissue), are not sufficient to optimize survival of the AAM over time. The short-term increase in graft weight at 4-week follow-up could relate to the presence of EVE-induced edema within the grafts, as suggested by the parallel increase in tissue inflammation. Differences between cross-sectional area assessments and outcomes observed in samples' weights might relate to the loss of tissue fluids (e.g., edema) during the processing of histological sections, so that the group with the highest weight resulted in the lowest cross-sectional area (highest loss of fluid-related weight).

During the third optimization set of experiments, we analyzed the effect of different densities of combined small AAM and autologous adipose tissue grafts to mimic a clinical scenario in which the AAM is not grafted as a ''standalone'' regenerative product, but is instead combined with autologous adipose tissue, aiming to improve graft survival.[12,13,29] Supplying additional ECM to autologous adipose tissue grafts has the potential to improve outcomes in clinical scenarios where a sufficient amount of autologous adipose tissue would be lacking (e.g., patients with a very low BMI or a low body fat percentage).

Our results showed that a varying density of combined small AAM and adipose tissue does not negatively affect adipocyte viability *in vitro* or *in vivo* (graft weight and volume). However, the combination of a low-density AAM (6.25% protein mass to saline ratio) and adipose tissue (50% ratio) provides the best ease of injection, control of graft placement, histological quality of the AAM (less cystic-like areas), angiogenesis (1.5-fold increase compared to control adipose tissue grafts), and adipogenesis. We believe these outcomes might be due to the easier migration of metabolites and cells (e.g., blood vessels) within a less dense graft, compared to more dense grafts.

Combinations of high-density AAM and adipose tissue led to a higher graft weight and cross-sectional area at follow-up, yet we postulate this finding might relate to the structural effect of the AAM itself (e.g., higher weight, higher quantity of ECM components in the graft), more than a biological phenomenon. Further research might need to assess if even lower AAM densities might further enhance outcomes.

Overall, this study has shown that combination of EVE and the AAM can best prepare tissues to receive tissue grafts. This effect can, as a consequence, enhance the survival of grafted autologous adipose tissue. Advantages of this new biomaterial include the following: (1) a widely available source of tissue (allogeneic and human donors), which allows scaling and manufacturing of an off-the-shelf scaffold, (2) the biomimetic (angiogenic and adipogenic) properties provided by a human-derived decellularized ECM, (3) the small-size scaffold and injectable configuration of the scaffold that allow easier clinical use in minimally invasive procedures, and (4) the minimal manipulation process to preserve the endogenous structural and biological components of the scaffold to support its natural function *in vivo*.

Yet, these outcomes have been obtained in a murine model and present a few limitations.

We do not have *in vitro* data on how the different scaffold sizes might affect the viability of adipose tissue.

In addition, our choice of using only female animals, despite being representative of the most common clinical population receiving adipose tissue grafts for reconstructive or aesthetic procedures, might have affected outcomes since the effects of female hormones on the physiology of adipose tissue have been well characterized. Future research will need to confirm and validate our outcomes also in male models.

The model used in the first two sets of experiments of this study featured a xenogeneic graft, which we assume might have further limited the regenerative properties of the AAM, compared to the allogenic scenario of a future clinical use. In addition, since the two preparations o the AAM were not grafted in the same animals (one per side), biological variability could have affected our outcomes.

Consistently, in the third set of experiments, the use of an immune-deficient animal model might have partially hindered the effects of immune response against the AAM grafts. The results obtained in immunocompetent mice for Study 1 and Study 2 might not have been completely extrapolated or replicated in this model with regard to the degree of inflammation, angiogenesis, and fat necrosis or resorption. The small sample size ($n = 5$ per group) might have further limited our capacity to draw significant outcomes. The inflammatory infiltrate around the graft, and the loss of ECM architecture in the central portion of the AAM grafts, might have limited the recruitment of adipocytes into the graft.

These results could be related to the large volume of grafted AAM (0.5 cc) with respect to the adopted murine model and in the fact that this represented a xenologous graft across species in immunocompetent recipient animals. We believe that the AAM's potential to assist adipogenesis in an allogeneic scenario is higher, but requires an interspersed proximity to a cellular milieu, which can be achieved by injecting adipose cells combined with AAM or smaller volumes of AAM.

Also, despite the AAM mimicks the normal adipose microenvironment, it does not perfectly replicate its conformation.

Despite a general similarity of the adipose tissue ECM in different body areas, the area from which the tissue for preparing the AAM was procured could have affected its biological properties, and further research is needed to determine the existence and impact of such differences.

In conclusion, our study demonstrates that combined use of cyclical EVE and AAM grafts with/without adipose tissue can create a vascularized, proadipogenic environment to assist long-term survival (volume retention) of autologous adipose tissue grafts in a murine model. In these experiments, the graft gradually decreased in size over time. Hence, further preclinical and clinical studies should confirm these findings by evaluating their direct effect on autologous adipose grafts.

This study provides initial guidance to improve clinical outcomes with the use of the AAM. In particular, despite this technology (AAM) being already clinically available and currently tested in clinical trials,[37] further preclinical optimization and clinical validation of all other variables related to the treatment (e.g., ideal grafted volume of AAM, differences in outcomes with varying grafted volumes of AAM, biological differences in AAM from different tissues of origin/donors, best method to combine the AAM to lipoaspirate, etc.) are necessary and will benefit more widespread application of the AAM in clinical practice.

Acknowledgments

The authors thank Marc Jacobs of the Musculoskeletal Transplant Foundation (MTF) for providing the Allograft Adipose Matrix. This study was funded through a grant from the MTF to Brigham and Women's Hospital and from a grant from the Gillian Reny Stepping Strong Foundation.

Submission Declaration

The work described in this article has not been published previously (except in the form of an abstract or as part of a published lecture or academic thesis, or as an electronic preprint) and is not under consideration for publication elsewhere. Its publication is approved by all authors and by the responsible authorities where the work was carried out, and, if accepted, it will not be published elsewhere in the same form, in English or in any other language, including electronically, without the written consent of the copyright-holder. This work has not been presented at scientific meetings.

Authorship

All authors had full access to the data of this study and take responsibility for its integrity and the accuracy of its analysis. All authors have seen and agreed to the submitted version of the article, bearing responsibility for it.

Authors' Contributions

G.G.: contributed to study concept and design, conducted experimental activities, analysis and interpretation of data, article drafting, and revision. J.S.: contributed to analysis and interpretation of data, article drafting, and revision. A.H., C.S., G.L., and X.W.: contributed to experimental activities, and analysis and interpretation of data. B.S. and E.C.: contributed to the design of the study, prepared the Allograft Adipose Matrix, and helped revise the article. H.M.: contributed to analysis, interpretation, and representation of data. D.P.O.: contributed to study concept and design, supervised the study, and provided critical revision of data and article.

Ethics

The displayed study was carried out with respect of high ethical standards. All the studies have been approved, when required, by the appropriate ethics committee and have, therefore, been performed in accordance and in conformity to the World Medical Association Declaration of Helsinki (June 1964) and subsequent amendments. All animal experiments have been designed and performed in accordance with the ARRIVE guidelines and the National Institutes of Health guide for the care and use of Laboratory animals (NIH Publications No. 8023, revised 1978).

Disclosure Statement

Dr. Orgill is a consultant for the Musculoskeletal Transplant Foundation (MTF) and receives research funding through grants to Brigham and Women's Hospital by MTF. E.C. is an employee of the MTF. All other authors declare no actual or potential conflict of interests: in addition, they disclose no commercial or financial associations, personal or other relationships, with other people or organizations that could inappropriately influence the reported article or create a conflict of interests with the information presented.

References

1. Coleman, S.R. Structural fat grafting: more than a permanent filler. Plast Reconstr Surg **118**(3 Suppl.), 108S, 2006.
2. Coleman, S.R. Structural fat grafting. Aesthet Surg J **18,** 386, 1998.
3. Agha, R.A., Fowler, A.J., Herlin, C., Goodacre, T.E.E., and Orgill, D.P. Use of autologous fat grafting for breast reconstruction: a systematic review with meta-analysis of oncological outcomes. J Plast Reconstr Aesthet Surg **68,** 143, 2015.
4. Eto, H., Kato, H., Suga, H., *et al.* The fate of adipocytes after nonvascularized fat grafting: evidence of early death and replacement of adipocytes. Plast Reconstr Surg **129,** 1081–1092, 2012.
5. Geissler, P.J., Davis, K., Roostaeian, J., Unger, J., Huang, J., and Rohrich, R.J. Improving fat transfer viability: the role of aging, body mass index, and harvest site. Plast Reconstr Surg **134,** 227, 2014.
6. Suga, H., Eto, H., Aoi, N., *et al.* Adipose tissue remodeling under ischemia: death of adipocytes and activation of stem/progenitor cells. Plast Reconstr Surg **126,** 1911, 2010.
7. Eto, H., Suga, H., Inoue, K., *et al.* Adipose injury-associated factors mitigate hypoxia in ischemic tissues through activation of adipose-derived stem/progenitor/stromal cells and induction of angiogenesis. Am J Pathol **178,** 2322, 2011.
8. Suga, H., Matsumoto, D., Inoue, K., *et al.* Numerical measurement of viable and nonviable adipocytes and other cellular components in aspirated fat tissue. Plast Reconstr Surg **122,** 103, 2008.
9. Heit, Y.I., Lancerotto, L., Mesteri, I., *et al.* External volume expansion increases subcutaneous thickness, cell proliferation, and vascular remodeling in a murine model. Plast Reconstr Surg **130,** 541, 2012.

10. Khouri, R.K., Rigotti, G., Khouri, R.K., *et al.* Tissue-engineered breast reconstruction with Brava-assisted fat grafting: a 7-year, 488-patient, multicenter experience. Plast Reconstr Surg **135,** 643, 2015.
11. Giatsidis, G., Cheng, L., Facchin, F., *et al.* Moderate-intensity intermittent external volume expansion optimizes the soft tissue response in a murine model. Plast Reconstr Surg **139,** 882, 2017.
12. Wang, L., Johnson, J.A., Zhang, Q., and Beahm, E.K. Combining decellularized human adipose tissue extracellular matrix and adipose-derived stem cells for adipose tissue engineering. Acta Biomater **9,** 8921, 2013.
13. Flynn, L.E. The use of decellularized adipose tissue to provide an inductive microenvironment for the adipogenic differentiation of human adipose-derived stem cells. Biomaterials **31,** 4715, 2010.
14. Flynn, L., Prestwich, G.D., Semple, J.L., and Woodhouse, K.A. Adipose tissue engineering with naturally derived scaffolds and adipose-derived stem cells. Biomaterials **28,** 3834, 2007.
15. Turner A.E., Yu, C., Bianco, J., Watkins, J.F., and Flynn, L.E. The performance of decellularized adipose tissue microcarriers as an inductive substrate for human adipose-derived stem cells. Biomaterials **33,** 4490, 2012.
16. Yu, C., Bianco, J., Brown, C., *et al.* Porous decellularized adipose tissue foams for soft tissue regeneration. Biomaterials **34,** 3290, 2013.
17. Han, T.T.Y., Toutounji, S., Amsden, B.G., and Flynn, L.E. Adipose-derived stromal cells mediate in vivo adipogenesis, angiogenesis and inflammation in decellularized adipose tissue bioscaffolds. Biomaterials **72,** 125, 2015.
18. Haddad, S.M.H., Omidi, E., Flynn, L.E., and Samani, A. Comparative biomechanical study of using decellularized human adipose tissues for post-mastectomy and post-lumpectomy breast reconstruction. J Mech Behav Biomed Mater **57,** 235, 2016.
19. Cheung, H.K., Han, T.T.Y., Marecak, D.M., Watkins, J.F., Amsden, B.G., and Flynn, L.E. Composite hydrogel scaffolds incorporating decellularized adipose tissue for soft tissue engineering with adipose-derived stem cells. Biomaterials **35,** 1914, 2014.
20. Compton, C.C., Butler, C.E., Yannas, I.V., Warland, G., and Orgill, D.P. Organized skin structure is regenerated *in vivo* from collagen-GAG matrices seeded with autologous keratinocytes. J Invest Dermatol **110,** 908, 1998.
21. Yannas, I.V., Lee, E., Orgill, D.P., Skrabut, E.M., and Murphy, G.F. Synthesis and characterization of a model extracellular matrix that induces partial regeneration of adult mammalian skin. Proc Natl Acad Sci U S A **86,** 933, 1989.
22. Climov, M., Bayer, L.R., Moscoso, A.V., Matsumine, H., and Orgill, D.P. The role of dermal matrices in treating inflammatory and diabetic wounds. Plast Reconstr Surg **138**(3 Suppl.), 148S, 2016.
23. Jansen, L.A., De Caigny, P., Guay, N.A., Lineaweaver, W.C., and Shokrollahi, K. The evidence base for the acellular dermal matrix AlloDerm: a systematic review. Ann Plast Surg **70,** 587, 2013.
24. Eweida, A.M., and Marei, M.K. Naturally occurring extracellular matrix scaffolds for dermal regeneration: do they really need cells? Biomed Res Int **2015,** 839694, 2015.
25. Omidi, E., Fuetterer, L., Reza Mousavi, S., Armstrong, R.C., Flynn, L.E., and Samani, A. Characterization and assessment of hyperelastic and elastic properties of decellularized human adipose tissues. J Biomech **47,** 3657, 2014.
26. Giatsidis, G., Dalla Venezia, E., Venezia, E.D., De Stefani, D., Rizzuto, R., and Bassetto, F. Breast tissue engineering: decellularized scaffolds derived from porcine mammary glands. Plast Reconstr Surg **136**(4 Suppl.), 35, 2015.
27. Yu, C., Kornmuller, A., Brown, C., Hoare, T., and Flynn, L.E. Decellularized adipose tissue microcarriers as a dynamic culture platform for human adipose-derived stem/stromal cell expansion. Biomaterials **120,** 66, 2017.
28. Brown, B.N., Freund, J.M., Han, L., *et al.* Comparison of three methods for the derivation of a biologic scaffold composed of adipose tissue extracellular matrix. Tissue Eng Part C Methods **17,** 411, 2011.
29. Banyard, D.A., Borad, V., Amezcua, E., Wirth, G.A., Evans, G.R.D., and Widgerow, A.D. Preparation, characterization, and clinical implications of human decellularized adipose tissue extracellular matrix (hDAM): a comprehensive review. Aesthet Surg J **36,** 349, 2016.
30. Roehm, K.D., Hornberger, J., and Madihally, S.V. *In vitro* characterization of acelluar porcine adipose tissue matrix for use as a tissue regenerative scaffold. J Biomed Mater Res A **104,** 3127, 2016.
31. Choi, Y.C., Choi, J.S., Kim, B.S., Kim, J.D., Yoon, H.I., and Cho, Y.W. Decellularized extracellular matrix derived from porcine adipose tissue as a xenogeneic biomaterial for tissue engineering. Tissue Eng Part C Methods **18,** 866, 2012.
32. Tan, Q.W., Zhang, Y., Luo, J.C., *et al.* Hydrogel derived from decellularized porcine adipose tissue as a promising biomaterial for soft tissue augmentation. J Biomed Mater Res A **105,** 1756, 2017.
33. Lin, C.-Y., Liu, T.-Y., Chen, M.-H., Sun, J.-S., and Chen, M.-H. An injectable extracellular matrix for the reconstruction of epidural fat and the prevention of epidural fibrosis. Biomed Mater **11,** 035010, 2016.
34. Zelen, C.M., Orgill, D.P., Serena, T.E., *et al.* Human reticular acellular dermal matrix in the healing of chronic diabetic foot ulcerations that failed standard conservative treatment: a retrospective crossover study. Wounds **29,** 39, 2017.
35. Sbitany, H., and Serletti, J.M. Acellular dermis-assisted prosthetic breast reconstruction: a systematic and critical review of efficacy and associated morbidity. Plast Reconstr Surg **128,** 1162, 2011.
36. RENUVA® allograft adipose matrix instructions for use read before using donated human tissue description and indications for use. Available at: https://www.mtf.org/documents/PI_113_REV_5.pdf (accessed April 19, 2018).
37. Shahin, T.B., Vaishnav, K.V., Watchman, M., *et al.* Tissue augmentation with allograft adipose matrix for the diabetic foot in remission. Plast Reconstr Surg Glob Open **5,** e1555, 2017.
38. Lancerotto, L., Chin, M.S., Freniere, B., *et al.* Mechanisms of action of external volume expansion devices. Plast Reconstr Surg **132,** 569, 2013.
39. Lujan-Hernandez, J., Lancerotto, L., Nabzdyk, C., *et al.* Induction of adipogenesis by external volume expansion. Plast Reconstr Surg **137,** 122, 2016.
40. Giatsidis, G., Cheng, L., Haddad, A., *et al.* Noninvasive induction of angiogenesis in tissues by external suction: sequential optimization for use in reconstructive surgery. Angiogenesis **21,** 61, 2018.

41. Thanik, V.D., Chang, C.C., Lerman, O.Z., *et al.* A murine model for studying diffusely injected human fat. Plast Reconstr Surg **124,** 74, 2009.
42. Louis, K.S., and Siegel, A.C. Cell viability analysis using trypan blue: manual and automated methods. Methods Mol Biol **740,** 7, 2011.
43. Wei, S., Orgill, D.P., and Giatsidis, G. Delivery of external volume expansion (EVE) through micro-deformational interfaces safely induces angiogenesis in a murine model of intact diabetic skin with endothelial cell dysfunction (ECD). Plast Reconstr Surg. 2018, In press.
44. Kato, H., Suga, H., Eto, H., *et al.* Reversible adipose tissue enlargement induced by external tissue suspension: possible contribution of basic fibroblast growth factor in the preservation of enlarged tissue. Tissue Eng Part A **16,** 2029, 2010.
45. Kato, H., Araki, J., Doi K., *et al*. Normobaric hyperoxygenation enhances initial survival, regeneration, and final retention in fat grafting. Plast Reconstr Surg **134,** 951, 2014.
46. Brown, C.F.C., Yan, J., Han, T.T.Y., Marecak, D.M., Amsden, B.G., and Flynn, L.E. Effect of decellularized adipose tissue particle size and cell density on adipose-derived stem cell proliferation and adipogenic differentiation in composite methacrylated chondroitin sulphate hydrogels. Biomed Mater **10,** 045010, 2015.
47. Khouri, R.K., Khouri, R.-E.R., Lujan-Hernandez, J.R., Khouri, K.R., Lancerotto, L., and Orgill, D.P. Diffusion and perfusion: the keys to fat grafting. Plast Reconstr Surg Glob Open **2,** e220, 2014.
48. Khouri, R.K., Rigotti, G., Cardoso, E., Khouri, R.K., and Biggs, T.M. Megavolume autologous fat transfer: part II. Practice and techniques. Plast Reconstr Surg **133,** 1369, 2014.
49. Gir, P., Brown, S.A., Oni, G., Kashefi, N., Mojallal, A., and Rohrich, R.J. Fat grafting: evidence-based review on autologous fat harvesting, processing, reinjection, and storage. Plast Reconstr Surg **130,** 249, 2012.
50. Coleman, S.R., and Katzel, E.B. Fat grafting for facial filling and regeneration. Clin Plast Surg **42,** 289, 2015.
51. Rao, A., and Saadeh, P.B. Defining fat necrosis in plastic surgery. Plast Reconstr Surg **134,** 1202, 2014.
52. Szade, A., Grochot-Przeczek, A., Florczyk, U., Jozkowicz, A., and Dulak, J. Cellular and molecular mechanisms of inflammation-induced angiogenesis. IUBMB Life **67,** 145, 2015.
53. Kwee, B.J., and Mooney, D.J. Manipulating the intersection of angiogenesis and inflammation. Ann Biomed Eng **43,** 628, 2015.
54. Morrison, W.A., Marre, D., Grinsell, D., Batty, A., Trost, N., and O'Connor, A.J. Creation of a large adipose tissue construct in humans using a tissue-engineering chamber: a step forward in the clinical application of soft tissue engineering. EBioMedicine **6,** 238, 2016.
55. Chin, M.S., Lujan-Hernandez, J., Babchenko, O., *et al.* External volume expansion in irradiated tissue: effects on the recipient site. Plast Reconstr Surg **137,** 799e, 2016.

Address correspondence to:
Giorgio Giatsidis, MD, PhD
Division of Plastic Surgery
Department of Surgery
Brigham and Women's Hospital
Harvard Medical School
75 Francis Street
Boston, MA 02115

E-mail: ggiatsidis@bwh.harvard.edu
or dr.giatsidis@gmail.com

Dennis Paul Orgill, MD, PhD
Tissue Engineering and Wound Healing Laboratory
Division of Plastic Surgery
Department of Surgery
Brigham and Women's Hospital
Harvard Medical School
75 Francis Street
Boston, MA 02115

E-mail: dorgill@bwh.harvard.edu

Received: February 13, 2018
Accepted: July 24, 2018
Online Publication Date: October 11, 2018

Appendix follows→

Appendix: Graphical Abstract

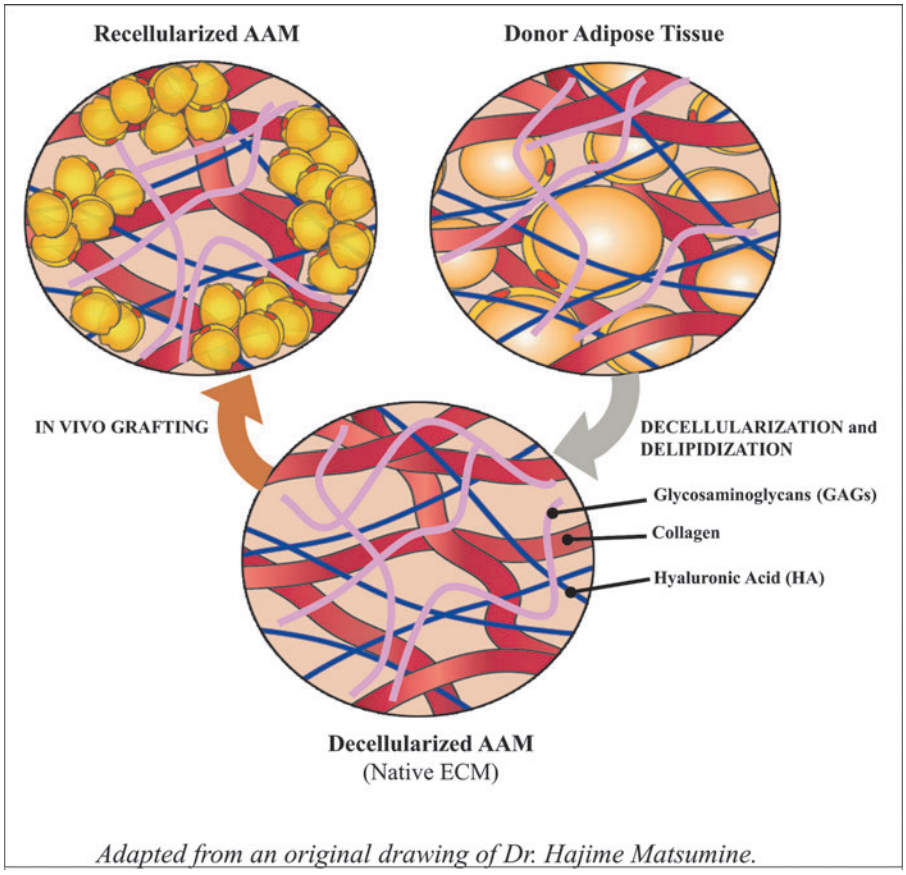

APPENDIX FIG. A1. Schematic representation of how adipose tissue (above, right) is processed to remove lipid and cell remnants to produce an Allograft Adipose Matrix (AAM) scaffold (below) that contains collagen, hyaluronic Acid (HA), and glycosaminoglycans (GAGs). The picture also shows how the decellularized AAM can be grafted *in vivo* to assist adipogenesis and adipose cell migration (above, left).